JCI The Journal of Clinical Investigation

Sodium- and energy-dependent uptake of myo-inositol by rabbit peripheral nerve. Competitive inhibition by glucose and lack of an insulin effect.

D A Greene, S A Lattimer

J Clin Invest. 1982;70(5):1009-1018. https://doi.org/10.1172/JCI110688.

Research Article

Experimental diabetes consistently reduces the concentration of free myo-inositol in peripheral nerve, which usually exceeds that of plasma by 90-100-fold. This phenomenon has been explicitly linked to the impairment of nerve conduction in the acutely diabetic streptozocin-treated rat. However, the mechanism by which acute experimental diabetes lowers nerve myo-inositol content and presumably alters nerve myo-inositol content and presumably alters nerve myo-inositol metabolism is unknown. Therefore, the effects of insulin and elevated medium glucose concentration of 2-[3H]myo-inositol uptake were studied in a metabolically-defined in vitro peripheral nerve tissue preparation derived from rabbit sciatic nerve, whose free myo-inositol content is reduced by experimental diabetes. The results demonstrate that myo-inositol uptake occurs by at least two distinct transport systems in the normal endoneurial preparation. A sodium- and energy-dependent saturable transport system is responsible for at least 94% of the measured uptake at medium myo-inositol concentrations approximating that present in plasma. This carrier-mediated transport system has a high affinity for myo-inositol (Kt = 63 microM), and is not influenced acutely by physiological concentrations of insulin; it is, however, inhibited by hyperglycemic concentrations of glucose added to the incubation medium in a primarily competitive fashion. Thus, competitive inhibition of peripheral nerve myo-inositol uptake by glucose may constitute a mechanism by which diabetes produces physiologically significant alterations in peripheral nerve myo-inositol metabolism.

Sodium- and Energy-dependent Uptake of *Myo*-inositol by Rabbit Peripheral Nerve

COMPETITIVE INHIBITION BY GLUCOSE AND LACK OF AN INSULIN EFFECT

DOUGLAS A. GREENE and SARAH A. LATTIMER, *Diabetes Research Laboratories of the Department of Medicine, School of Medicine, University of Pittsburgh, Pittsburgh, Pennsylvania 15261*

ABSTRACT Experimental diabetes consistently reduces the concentration of free *myo*-inositol in peripheral nerve, which usually exceeds that of plasma by 90–100-fold. This phenomenon has been explicitly linked to the impairment of nerve conduction in the acutely diabetic streptozocin-treated rat. However, the mechanism by which acute experimental diabetes lowers nerve *myo*-inositol content and presumably alters nerve *myo*-inositol metabolism is unknown. Therefore, the effects of insulin and elevated medium glucose concentration on 2-[^{3}H]*myo*-inositol uptake were studied in a metabolically-defined in vitro peripheral nerve tissue preparation derived from rabbit sciatic nerve, whose free *myo*-inositol content is reduced by experimental diabetes. The results demonstrate that *myo*-inositol uptake occurs by at least two distinct transport systems in the normal endoneurial preparation. A sodium- and energy-dependent saturable transport system is responsible for at least 94% of the measured uptake at medium *myo*-inositol concentrations approximating that present in plasma. This carrier-mediated transport system has a high affinity for *myo*-inositol (K_t = 63 μM), and is not influenced acutely by physiological concentrations of insulin; it is, however, inhibited by hyperglycemic concentrations of glucose added to the incubation medium in a primarily competitive fashion. Thus, competitive inhibition of peripheral nerve *myo*-inositol uptake by glucose may constitute a mechanism by which diabetes produces physiologically significant alterations in peripheral nerve *myo*-inositol metabolism.

Received for publication 14 December 1981 and in revised form 27 May 1982.

INTRODUCTION

Metabolic abnormalities in peripheral nerve resulting from chronic insulin deficiency and/or hyperglycemia are thought to influence heavily the development of diabetic neuropathy. Whether the major influence is mediated directly by deficient insulin action on peripheral nerve or indirectly by altered patterns of circulating metabolites is unresolved. Contrary to previous views (1, 2), circulating insulin does not primarily regulate peripheral nerve glucose and energy metabolism (3). Consequently, experimental diabetes does not impair glucose-derived energy production in peripheral nerve (4) although subtle insulin-sensitive metabolic perturbations in diabetic peripheral nerve have been described (4, 5). Recent attention has focussed on possible direct pathogenetic effects of hyperglycemia on peripheral nerve metabolism (6, 7). Both increased polyol (sorbitol) pathway activity and nonenzymatic protein-glycosylation occur in many tissues, including peripheral nerve, as a consequence of elevated ambient glucose concentration (8–14). The relationship, however, between these metabolic abnormalities in peripheral nerve and alterations in tissue structure or function is entirely obscure (7).

In contrast, although altered sciatic nerve *myo*-inositol metabolism in experimental diabetes has been explicitly linked to impairment of nerve conduction (15, 16), the mechanism(s) by which experimental diabetes lowers nerve *myo*-inositol content and alters nerve *myo*-inositol metabolism is entirely unclear at present (17, 18). In contrast to most other carbohydrates, *myo*-inositol is maintained at high intracellular concentrations by most tissues. Both endogenous synthesis from glucose and active concentration from

plasma have been invoked to explain this phenomenon (19, 20). Active concentration of *myo*-inositol has been described in kidney (21), small intestine (22), choroid plexus (23), ciliary body (24), and ocular lens (25). It has been postulated (17), but never demonstrated, in peripheral nerve (20). Although *myo*-inositol synthesis has been observed in crude homogenates of peripheral nerve (26), the relative importance of active concentration, intracellular sequestration (20), and endogenous synthesis in the maintenance of nerve *myo*-inositol concentrations is unknown (17, 18, 20). In the studies presented here, we demonstrate that *myo*-inositol uptake occurs in endoneurial tissue via a sodium- and energy-dependent, ouabain-inhibitable, high affinity, carrier mediated transport system. Hyperglycemic concentrations of glucose competitively inhibit carrier-mediated *myo*-inositol uptake, and may hereby contribute to the reduction of nerve *myo*-inositol content in experimental diabetes.

METHODS

In vitro peripheral nerve preparations. Endoneurial preparations were derived from the tibial division of rabbit sciatic nerve as previously described (27). Male white New Zealand rabbits weighing 1.5–2.0 kg were maintained on Wayne Rabbit Ration (free *myo*-inositol content, 0.04% wt/wt) and were fasted overnight before study (fasting plasma *myo*-inositol concentration, 21.2±2.4 μM, $n = 16$). After sedation (diazepam 2 mg/kg i.m.) and induction of anesthesia (sodium pentabarbital 24–36 mg/kg i.v.), a defined segment of each sciatic nerve was surgically exposed, ligated, removed with preservation of hemostasis, and transferred to a 125-ml Erlenmeyer flask containing 70 mg of collagenase (Type I, Sigma Chemical Co., St. Louis, MO) dissolved in 10 ml of 4.5% dialyzed defatted (28) bovine serum albumin (BSA) (Sigma fraction V powder, Sigma Chemical Co.) and 20 mM glucose in Krebs Ringer bicarbonate buffer medium (KRB),[1] pH 7.4, equilibrated with 5% CO_2/95% O_2 at 37°C. After controlled digestion for 12–14 min, the nerve segments were rinsed in 30 ml of similar medium containing apoprotinin, 200 Kallikrein Inactivation U/ml (Trasylol, FBA Pharmaceuticals, New York). A branch-free segment of the major fascicle of the tibial division of each sciatic nerve was ligated and microdissected to produce the endoneurial preparation (27).

Standard incubation medium for the endoneurial preparation was 4.5% dialyzed defatted BSA and 5 mM glucose in KRB, pH 7.4, equilibrated with 5% CO_2/95% O_2. In contrast to previously published studies with the endoneurial preparation, *myo*-inositol was absent from the standard incubation medium.

In the initial characterization of the endoneurial preparation, 500 μM medium *myo*-inositol was necessary to prevent slow declines in oxygen uptake and tissue *myo*-inositol concentration (27), but these initial studies were performed before fraction V BSA was routinely defatted before use. Charcoal treatment (28) of fraction V BSA obviates the requirement for *myo*-inositol in the medium.[2] This observation was confirmed in this laboratory as well: after paired endoneurial preparations were incubated for 2 h under standard conditions either in the presence or absence of 500 μM *myo*-inositol, oxygen uptake was 27.4±2.2 and 25.0±2.2 mmol/kg per h, respectively (mean Δ of paired samples −2.3±1.5 mmol/kg per h, $n = 5$, $0.4 > P > 0.2$). The reduction in endoneurial tissue *myo*-inositol after incubation with the *myo*-inositol-free medium was shown to be the result of extracellular loss: paired samples of the endoneurial preparation were incubated in standard medium with or without 500 μM *myo*-inositol; 1-[^{14}C]mannitol was added as a marker of extracellular space. Extracellular *myo*-inositol concentration was presumed to be negligible in tissue samples incubated in *myo*-inositol-free medium and equal to 500 μM in samples incubated with *myo*-inositol. Intracellular *myo*-inositol was 3.46±0.30 mmol/kg and 3.53±0.21 mmol/kg in samples incubated with and without *myo*-inositol, respectively (mean Δ of paired samples +0.07±0.13 mmol/kg, $n = 6$, $1.0 > P > 0.5$).

Label uptake experiments. The endoneurial preparation was routinely preincubated in 3 ml of standard medium in a 10-ml Erlenmeyer flask in a Dubnoff metabolic shaker set at 88 cycles/min and 37°C. The preincubated endoneurial preparation was transferred to a new flask containing standard medium with 1 μCi/ml of 2-[^{3}H]*myo*-inositol at the desired medium *myo*-inositol concentration and 0.5 μCi/ml of 1-[^{14}C]mannitol, 45 mCi/mmol (New England Nuclear, Boston, MA). To assess the effects of sodium ion in the extracellular fluid on *myo*-inositol uptake, sodium was replaced by equimolar concentrations of choline during the last 15 min of preincubation and during the exposure to isotopically labeled compounds. Sodium-dependent 2-[^{3}H]*myo*-inositol uptake was taken as the difference in intracellular uptake by tissue in the presence or absence of sodium under each experimental condition. Other experimental modifications in the incubation conditions for specific studies are described in the relevant portions of the text, tables, and figures.

After brief, timed exposure to isotopically-labeled medium, the endoneurial preparation was rapidly rinsed in *myo*-inositol-free standard medium, and frozen in liquid nitrogen that had been evacuated to its freezing point (29). The frozen endoneurial preparation was rapidly weighed on a microbalance, powdered in liquid nitrogen, and homogenized in 6% perchloric acid as previously described (27). Incubation medium was quantitatively transferred to a volumetric flask and made to a 5-ml vol with water. Aliquots were deproteinized with equal volumes of 12% perchloric acid. After centrifugation at 2,500 *g* for 15 min at 4°C, the supernatant of the tissue or medium perchloric acid extract was neutralized with KOH and recentrifuged. A 0.4-ml aliquot of the resulting supernatant was added to 15 ml of Aquasol II (New England Nuclear) and counted for ^{3}H and ^{14}C in a liquid scintillation spectrometer (Packard Tri-Carb, Packard Instrument Co., Downers Grove, IL) with automatic external standard ratios to correct for quenching. Cross-over of ^{14}C and ^{3}H radioactivity was determined at varying automatic external standard ratios in vials containing varying amounts of acetone in water as a quenching agent. Recovery of 2-[^{3}H]*myo*-inositol added to nerve homogenates was >93% on a volume basis when compared with recovery after neu-

[1] *Abbreviations used in this paper*: KRB, Krebs Ringer bicarbonate buffer; K_t, the substrate concentration at which the initial velocity is one-half of V_{max}; K_i, transport inhibitor constant; NEM, *N*-ethylmaleimide; V_{max}, maximum initial velocity.

[2] Personal communication, Albert I. Winegrad, University of Pennsylvania.

tralization and centrifugation of 2-[^{3}H]*myo*-inositol added to 6% perchloric acid.

The extracellular tissue space in milliliters per gram wet weight was calculated as dpm ^{14}C/g wet wt of tissue/dpm ^{14}C/ml incubation medium.

The tissue water-soluble ^{3}H was partially characterized by lyophilization and column chromatography. Pooled neutralized perchloric acid tissue extracts were applied to a 6 g × 15 mm column of AG-501-X8 mixed-bed resin (Bio-Rad Laboratories, Richmond, CA) with 5 μmol of unlabeled carrier *myo*-inositol and mannitol and eluted to 50 ml with distilled water. The effluent was pooled, lyophilized, reconstituted in 2 ml of water, and counted in 15 ml of Aquasol II for ^{3}H and ^{14}C. After correction for recovery of ^{14}C or for the recovery of pure 2-[^{3}H]*myo*-inositol applied to the column, >97% of the ^{3}H label was recovered from the column. In separate studies, the column retained >95% of *myo*-inositol-1P and *myo*-inositol-2P when eluted with 50 ml of water and assayed by the method of Barnett et al. (30). Both phosphorylated derivatives were easily eluted by 5 N NaOH.

To assess high affinity tissue *myo*-inositol binding, endoneurial preparations were homogenized in 59 mM potassium phosphate buffer containing 0.3 M sucrose and 2.5 mM EDTA, and treated with charcoal (Norit A, Fisher Scientific Co., Pittsburgh, PA) as described by Peach and Russell (31). Supernatants were prepared by centrifugation, incubated for up to 24 h at room temperature in the presence and absence of 2.5 mM magnesium with 2-[^{3}H]*myo*-inositol, and then chromatographed over G-25 Sephadex (Pharmacia Fine Chemicals, Piscataway, NJ). Aliquots of the column effluent were added to Aquasol II and counted for ^{3}H. No significant binding of 2-[^{3}H]*myo*-inositol was detectable.

To estimate the proportion of 2-[^{3}H]*myo*-inositol incorporated into nonwater soluble fractions, endoneurial preparations were incubated under standard conditions with 5 μM *myo*-inositol and 5 mM glucose for 10 min. The nerves were digested in 1.0 ml Protosol (New England Nuclear) at 37°C and counted for ^{3}H and ^{14}C. Total incorporation of 2-[^{3}H]*myo*-inositol, corrected for medium contamination, was not significantly greater than water soluble ^{3}H. Incorporation of 2-[^{3}H]*myo*-inositol into total lipids was assessed in separate experiments. After incubation for 10 min in medium containing 5 mM glucose and 5 μM 2-[^{3}H]*myo*-inositol, endoneurial preparations were homogenized in 6% perchloric acid and centrifuged as usual. The supernatant was neutralized and counted for both ^{3}H and ^{14}C for determination of saturable *myo*-inositol uptake. The perchloric acid precipitate was extracted with calcium containing neutral and acidified chloroform methanol (32), and the extracts were washed with appropriate upper phase (33), pooled, evaporated under nitrogen in scintillation vials, and counted for ^{3}H in 15 ml of Aquasol II.

Analytical methods. Tissue, diet, and plasma *myo*-inositol were measured by gas-liquid chromatography as previously described (15). Tissue P-creatine was measured by an enzymatic spectrofluorometric technique (34). Oxygen uptake was measured polarographically in a YSI Oxygen Monitor model 53 (Yellow Springs Instrument Co., Yellow Springs, OH) as previously described (27). Reagents and standards were purchased from Sigma Chemical Co., unless otherwise stated, and were of the highest available purity. Gas-liquid chromatographic analysis of the glucose used in these studies demonstrated no detectable *myo*-inositol peak. Monocomponent porcine insulin was a generous gift of Dr. Mary A. Root of the Eli Lilly Co., Indianapolis, IN. Dr. Carol Coffee of the Department of Biochemistry, School of Medicine, University of Pittsburgh, generously supplied purified *myo*-inositol-1-phosphate and *myo*-inositol-2-phosphate.

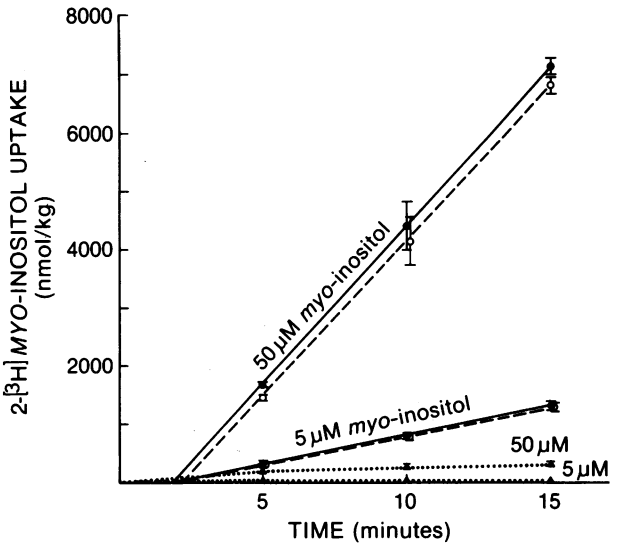

FIGURE 1 Endoneurial intracellular 2-[^{3}H]*myo*-inositol uptake as a function of time. Endoneurial preparations were isolated, preincubated for 1 h, and exposed to 2-[^{3}H]*myo*-inositol in the presence of 1-[^{14}C]mannitol and 5 mM glucose for varying time periods as described in Table II and Methods. Tritium and ^{14}C radioactivities were measured in deproteinized, neutralized perchloric acid extracts of tissue rapidly frozen in liquid nitrogen after incubation, and in medium samples. Intracellular 2-[^{3}H]*myo*-inositol uptake was calculated on the basis of the tissue ^{3}H content corrected for extracellular medium contamination by the [^{14}C]mannitol space, and expressed in terms of wet weight of the tissue and the specific activity of medium 2-[^{3}H]*myo*-inositol. 2 [^{3}H]*myo*-inositol uptake was measured in the presence (solid lines) or absence (dotted lines) of 144 mM sodium at 5 and 50 μM medium *myo*-inositol. Sodium-dependent uptake (dashed lines) was calculated as the difference between uptake in the presence and absence of sodium at each time point. Error bars indicate ±SEM; and the lines of best fit were derived by the method of least squares. Each data point represents the mean of at least four determinations.

Statistical methods. Data were calculated as mean±SEM. Significance of difference between groups was analyzed by the Student's two-tailed *t* test (35). The differences between paired samples were analyzed by the *t* test for paired comparisons (35). Kinetic analysis of 2-[^{3}H]*myo*-inositol uptake was performed by the Eadie-Hofstee and Lineweaver-Burk transformations of the Michaelis-Menten equation. The inhibitor constant for glucose ($K_{[glucose]}$)was estimated by the Dixon convention. Linear regression analysis was performed by the method of least squares (35).

RESULTS

Intracellular uptake of 2-[^{3}H]*myo*-inositol by the endoneurial preparation at 5 μM *myo*-inositol and in the presence of 5 mM glucose and physiological concentrations of sodium increased linearly with respect to time for 15 min after a 1-h preincubation (Fig. 1, lower solid line). This pattern was unaltered when the period of preincubation was increased to 2 h (data not shown).

Substitution of sodium ion in the KRB with equimolar concentrations of choline ion during the last 15 min of preincubation and during exposure to 5 μM 2-[^{3}H]*myo*-inositol reversibly abolished intracellular ^{3}H uptake (Fig. 1, lower dotted line). At higher medium *myo*-inositol concentrations (e.g., 50 μM), detectable intracellular 2-[^{3}H]*myo*-inositol uptake in the absence of sodium was nonlinear with respect to time (Fig. 1, upper dotted line). However, the differences between uptake in the presence and absence of sodium, i.e., the sodium-dependent uptake, were linear with respect to time for 15 min (Fig. 1, upper and lower dashed lines). Therefore, 10-min incubations with 2-[^{3}H]*myo*-inositol were chosen to estimate initial rates of sodium-dependent *myo*-inositol uptake under various incubation conditions after preincubation periods ranging from 1 to 2 h.

The mean composite (sodium-dependent plus independent) intracellular 2-[^{3}H]*myo*-inositol uptake rate during 10-min incubations in the presence of sodium was measured at medium *myo*-inositol concentrations ranging over three orders of magnitude to detect the presence of a saturable transport component. The mean 10-min composite uptake rate increased progressively over the concentration range tested (Fig. 2, solid line). The rate increased linearly with medium *myo*-inositol concentration from 0.8 to 16 μM, with a correlation coefficient (r) of 0.999 and a slope of 17.3 nmol/kg per min per μM. Partial saturation occurred between 16 and 200 μM *myo*-inositol. Thereafter, mean 10-min composite uptake increased linearly with medium *myo*-inositol concentration to the highest level tested (5,000 μM), but with a much lower slope (0.675 nmol/kg per min per μM, r = 0.990, Fig. 2, solid line). These data suggested that composite uptake was comprised of at least two distinct transport components, one with a high affinity for *myo*-inositol that became fully saturated within the concentration range tested, and one with a lower affinity for *myo*-inositol that demonstrated little or no saturation over the concentration range tested.

The mean 10-min intracellular 2-[^{3}H]*myo*-inositol uptake rate in the absence of extracellular sodium was directly proportional to medium *myo*-inositol concentration over the entire range tested (r = 0.991, slope = 0.529 nmol/kg per min per μM, Fig. 2, dotted line), which suggests that this process was unsaturable. In contrast, the initial rate of sodium-dependent 2-[^{3}H]*myo*-inositol uptake increased linearly with medium *myo*-inositol concentration only to 16 μM *myo*-inositol (r = 0.999, slope 16.8 nmol/kg per min per μM) and completely saturated below 5,000 μM *myo*-inositol (Fig. 2, dashed line). Therefore, 2-[^{3}H]*myo*-inositol uptake was considered to consist of two transport components, one sodium-dependent and saturable, and the other sodium-independent and unsaturable within the concentration range tested.

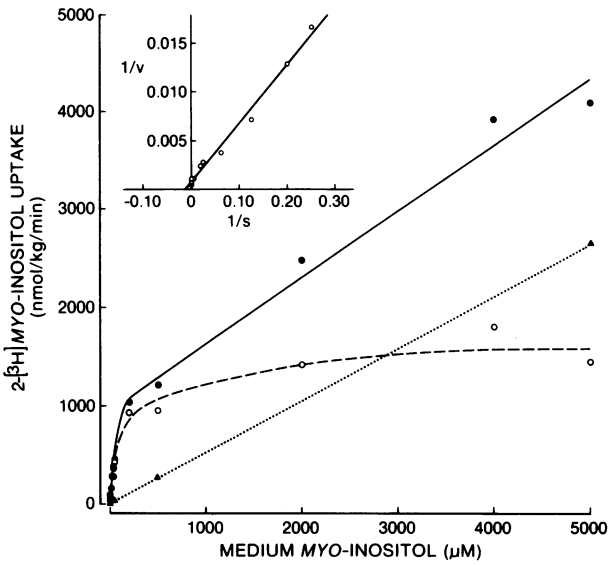

FIGURE 2 Mean 10-min rate of intracellular 2-[^{3}H]*myo*-inositol uptake by the endoneurial preparation as a function of medium *myo*-inositol concentration. Intracellular 2-[^{3}H]*myo*-inositol uptake was measured at varying medium *myo*-inositol concentrations after 10-min incubations as described in the previous figure in the presence (solid line, filled circles) or absence (dotted line, triangles) of sodium. Sodium-dependent uptake (dashed line, open circles) was computed by subtracting the uptake in sodium-free medium from the composite uptake measured in the presence of sodium. Inset shows sodium-dependent uptake plotted in double reciprocal fashion (Lineweaver-Burk transformation). Each point represents the mean of at least three determinations. Medium glucose concentration was 5 mM.

When sodium-dependent uptake and medium *myo*-inositol concentration were plotted as their double reciprocals (Fig. 2, inset), or when uptake velocity was plotted as a function of the ratio of uptake velocity to medium *myo*-inositol concentration (Eadie-Hofstee transformation, Fig. 3, middle panel), linear relationships were generated (r = 0.995 and 0.922, respectively). By the Lineweaver-Burk transformation of the double reciprocal plot, the apparent substrate concentration (K_t) was 88.9 μM and the apparent maximum initial velocity of transport (V_{max}) was 1,450 nmol/kg per min in the presence of 5 mM glucose. The Eadie-Hofstee transformation of the Michaelis-Menten equation yielded values of 82.5 μM and 1,390 nmol/kg per min for K_t and V_{max}, respectively. These kinetic data suggested that sodium-dependent 2-[^{3}H]*myo*-inositol uptake conformed to Michaelis-Menten kinetics, hereby implying that this uptake process represented carrier-mediated transport.

Since carrier-mediated transport systems are characteristically highly stereospecific, the ability of struc-

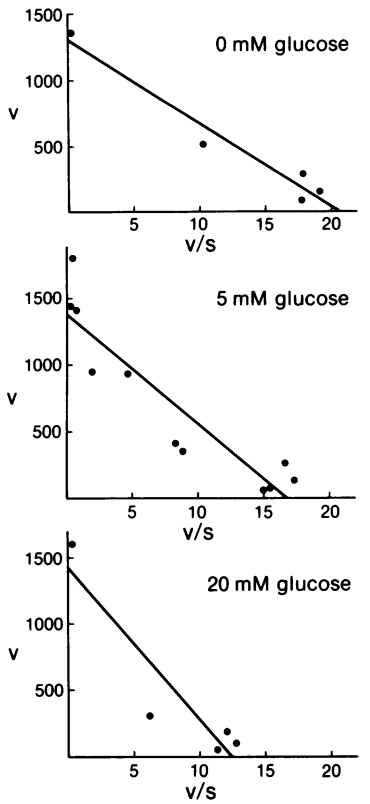

FIGURE 3 Sodium-dependent intracellular 2-[^{3}H]*myo*-inositol uptake as a function of the ratio of uptake velocity to medium *myo*-inositol concentration (Eadie-Hofstee convention) at 0 mM (top panel), 5 mM (middle panel), and 20 mM (bottom panel) medium glucose concentration. Sodium-dependent uptake was assessed as described in the preceding figure. Each data point represents the mean of at least three determinations. v, rate of sodium-dependent 2-[^{3}H]*myo*-inositol uptake (nanomoles per kilogram per minute); s, medium *myo*-inositol concentration (micromolars).

turally similar D-glucose to inhibit sodium-dependent 2-[^{3}H]*myo*-inositol uptake was assessed. When compared with uptake in physiological glucose concentrations (5 mM), sodium-dependent 2-[^{3}H]*myo*-inositol uptake in 20 mM glucose was reduced by 27 and 26% at medium *myo*-inositol concentrations of 5 and 50 μM, respectively (Tables I and II). Sodium-dependent *myo*-inositol uptake was not reduced by 20 mM glucose when medium *myo*-inositol concentration was 5,000 μM, i.e., >50 times the apparent K_t (Fig. 3, points nearest the vertical axis).

The Eadie-Hofstee plot of sodium-dependent 2-[^{3}H]-*myo*-inositol uptake and medium *myo*-inositol concentration in the presence of 20 mM glucose was linear (r = 0.921, Fig. 3, lower panel). The apparent V_{max} was 1,420 nmol/kg per min, but the apparent K_t with 20 mM glucose was 38.2% higher than at 5 mM glucose (Table III).

Sodium-dependent uptake was assessed at several concentrations of *myo*-inositol in the absence of glucose. Preliminary experiments demonstrated that significant decreases in tissue ATP and P-creatine were not detectable in the endoneurial preparation after 10-min incubations in the absence of substrate. The Eadie-Hofstee plot of sodium-dependent 2-[^{3}H]*myo*-inositol uptake was linear in the absence of glucose (r = 0.976, Fig. 3, upper panel). The apparent V_{max} was 1,310 nmol/kg per min, but the apparent K_t of 63.3 μM without glucose was lower than that at 5 or 20 mM glucose (Table III).

Thus, increasing medium glucose concentration was associated with progressively higher values for apparent K_t without similar increases in apparent V_{max}. Dixon plots of sodium-dependent uptake at 5, 8, 16, and 50 μM *myo*-inositol yielded a consistent apparent $K_{i(glucose)}$ of 37.8±2.2 (n = 6) (Fig. 4). These data are consistent with the hypothesis that glucose competed with 2-[^{3}H]*myo*-inositol for the transport carrier with an apparent K_i of ~38 mM (Table I). However, subtle noncompetitive components to the interaction of medium glucose and 2-[^{3}H]*myo*-inositol uptake cannot be rigorously excluded by the currently available data.

Sodium-dependent 2-[^{3}H]*myo*-inositol uptake was

TABLE I
Endoneurial Sodium-dependent 2-[^{3}H]Myo-inositol Uptake (Medium Myo-inositol Concentration 5 μM)

Incubation conditions	Sodium-dependent uptake	*P* vs. 5 mM, glucose alone
	nmol/kg/min	
5 mM glucose	77.5±3.8 (28)	—
20 mM glucose	56.6±3.2 (8)	<0.001
20 mM fructose	74.7±7.0 (6)	NS
20 mM mannitol	81.9±11.2 (6)	NS
No substrate	88.7±9.6 (6)	NS
0.1 mM NEM*	76.6±7.0 (6)	NS
1.0 mM NEM*	72.4±2.4 (6)	NS
Nitrogen atmosphere*‡	55.2±6.4 (5)	<0.005
2 mM Ouabain*	40.8±5.1 (6)	<0.001
100 μU/ml Insulin*	71.8±7.0 (5)	NS

Endoneurial preparations from rabbit sciatic nerve were isolated and preincubated as described in Methods. After 10-min exposure to 5 μM 2-[^{3}H]*myo*-inositol under the incubation conditions noted above, tissue water-soluble ^{3}H content was measured and then corrected for both extracellular medium contamination (by the [^{14}C]mannitol tissue space) and for sodium-independent intracellular 2-[^{3}H]*myo*-inositol accumulation as detailed in Methods. Results are expressed as mean±SEM, bracketed figures denote number of experiments, and *P* values are calculated on the basis of the Student's *t* test.

* 5 mM glucose present as substrate.

‡ Gas phase 95% N_2/5% CO_2.

TABLE II
Endoneurial Sodium-dependent 2-[^{3}H]Myo-inositol Uptake (Medium Myo-inositol Concentration 50 μM)

Incubation conditions	Sodium-dependent uptake	*P* vs. 5 mM, glucose alone
	nmol/kg/min	
5 mM Glucose	415±43 (9)	—
20 mM Glucose	310±15 (9)	<0.05
1.0 mM NEM*	446±25 (6)	NS
1,000 μU/ml Insulin*‡	390±41 (5)	NS

Endoneurial tissue preparations were isolated and preincubated as described in Table I. Following 10-min exposure to 50 μM 2-[^{3}H]*myo*-inositol under the incubation conditions noted above, tissue water-soluble ^{3}H content was measured, corrected for extracellular medium contamination and sodium-independent intracellular uptake, and expressed as in the previous table.
* 5 mM glucose present as substrate.
‡ Insulin was present both during the incubation with 2-[^{3}H]*myo*-inositol and in the preceding 1-h preincubation.

assessed in the presence of 20 mM fructose or 20 mM mannitol, two related compounds with molecular weights similar to that of glucose. Sodium-dependent uptake in 20 mM concentrations of fructose or mannitol was similar to uptake in the presence of 5 mM glucose, and greater than that which occurred in the presence of 20 mM glucose (Table II). Thus, neither fructose nor mannitol demonstrated the inhibitory effect of glucose on sodium-dependent uptake of 5 μM *myo*-inositol. (In contrast, sodium-dependent uptake was not influenced by medium glucose, fructose, or mannitol [data not shown]).

The reversibility of 2-[^{3}H]*myo*-inositol uptake at 5 and 5,000 μM *myo*-inositol was assessed. At these concentrations, 97 and 35%, respectively, of total intracellular uptake could be attributed to the sodium-dependent component. After 15 min of labeling with 2-[^{3}H]*myo*-inositol and [^{14}C]mannitol in the presence of sodium and 5 mM glucose, tissue radioactivity was compared in paired endoneurial samples either before or after a 10-min washout in *myo*-inositol-free medium. Results were expressed as the percentage change in total and intracellular 2-[^{3}H]*myo*-inositol during the washout. When endoneurial preparations were labeled in the presence of sodium at 5 μM *myo*-inositol, approximately one-quarter of the total tissue ^{3}H was lost during the subsequent 10-min washout (mean Δ of paired samples = −28.7±3.6%, $n = 6$, $P < 0.005$). However, when tissue ^{3}H was corrected for contaminating 2-[^{3}H]*myo*-inositol remaining in the mannitol (extracellular) space, the mean Δ was +25.4±13.7%, $n = 6$, $0.2 > P > 0.1$. Thus, intracellular 2-[^{3}H]*myo*-inositol uptake occurring primarily by the sodium-dependent system was largely irreversible (and may have continued during incubation in label-free media). In contrast, when 2-[^{3}H]*myo*-inositol was introduced into the tissue in the presence of sodium at a medium *myo*-inositol concentration of 5,000 μM, 80.1±0.9% of total and 42.7±12.2% of intracellular ^{3}H was lost during the subsequent 10-min washout ($n = 5$, $P < 0.001$ and $P < 0.05$, respectively). Thus, 2-[^{3}H]*myo*-inositol introduced into the tissue primarily via the sodium-independent transport component equilibrated more rapidly and/or to a much greater extent with the surrounding incubation medium than did label entering the tissue by the sodium-dependent uptake component.

Sensitivity to sulfhydryl reducing agents is characteristic of some carrier-mediated transport systems, including that described for *myo*-inositol in choroid plexus (36). The sensitivity of sodium-dependent endoneurial 2-[^{3}H]*myo*-inositol uptake to 0.1 and 1.0 mM *N*-ethylmaleimide (NEM) was measured in the presence of 5 mM glucose and at *myo*-inositol concentrations well below and near the apparent K_t (5 and 50 μM). In neither case did the presence of NEM alter 2-[^{3}H]*myo*-inositol uptake (Tables I and II).

To assess energy dependence, sodium-dependent 2-[^{3}H]*myo*-inositol uptake was measured in the presence of a 95% nitrogen atmosphere in medium containing 5 μM *myo*-inositol and 5 mM glucose. Sodium-dependent uptake was reduced by ~30% (Table II). Tissue P-creatine concentrations were reduced by 83% from 1.54±0.15 to 0.26±0.09 mmol/kg (mean Δ of paired samples = −1.29±0.12 mmol/kg, $n = 5$, $P < 0.005$) during the 10-min exposure to nitrogen.

Ouabain sensitivity of sodium-dependent 2-[^{3}H]*myo*-

TABLE III
Estimates of Kinetic Parameters of Sodium-dependent 2-[^{3}H]Myo-inositol Uptake by the Endoneurial Preparation

Medium glucose	V_{max}	K_t	*r*	*n**
mM	*nmol/kg/min*	*μM*		
Lineweaver-Burk analysis				
5	1,450	88.9	0.995	11
Eadie-Hofstee analysis				
0	1,310	63.3	0.976	5
5	1,390	82.5	0.922	11
20	1,420	114	0.921	5

Sodium-dependent 2-[^{3}H]*myo*-inositol uptake was measured and analyzed as described in the preceding tables. Kinetic parameters were estimated graphically by linear regression analysis as described in Methods. By Dixon analysis, $K_{i(glucose)}$ was 37.8±2.2 mM.
* Number of data points.

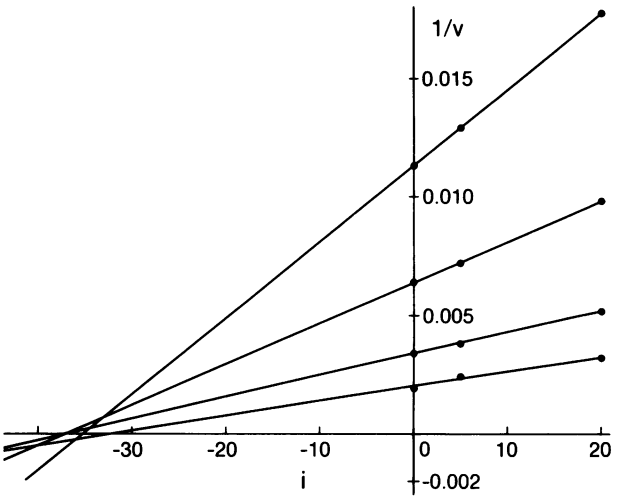

FIGURE 4 Graphic evaluation of $K_{i(glucose)}$ for sodium-dependent 2-[^{3}H]*myo*-inositol uptake by the Dixon plot. The reciprocal of sodium-dependent 2-[^{3}H]*myo*-inositol uptake measured at medium *myo*-inositol concentrations of 5, 8, 16, and 50 μM *myo*-inositol (top to bottom lines) were plotted as a function of medium glucose concentration. According to the Dixon convention, the intersection of each pair of linear regression lines for different *myo*-inositol concentrations constitutes an estimate of the $K_{i(glucose)}$. v, rate of sodium-dependent 2-[^{3}H]*myo*-inositol uptake; (nanomoles per kilogram per minute) i, medium glucose concentration (millimolars).

inositol uptake was assessed. In the presence of 5 mM glucose, 144 mM sodium, and 5 μM *myo*-inositol, 2 mM ouabain inhibited sodium-dependent 2-[^{3}H]*myo*-inositol uptake by 48% (Table II). A similar degree of inhibition occurred when sodium was present in the medium during preincubation, but was replaced by choline only during the labeling period (data not shown).

Sodium-dependent 2-[^{3}H]*myo*-inositol uptake was measured in the presence of insulin, 100 μU/ml, in medium containing 5 μM *myo*-inositol and 5 mM glucose. In a separate set of experiments, 1,000 μU/ml insulin was present both during the 1-h preincubation and during the exposure of the tissue to 50 μM 2-[^{3}H]*myo*-inositol in 5 mM glucose. In neither experiment did the presence of insulin alter the apparent rate of sodium-dependent 2-[^{3}H]*myo*-inositol uptake (Tables II and III). Neither insulin nor NEM altered sodium-independent uptake (data not shown).

During a 10-min incubation in 5 μM 2-[^{3}H]*myo*-inositol and 5 mM glucose, 2-[^{3}H]*myo*-inositol incorporation into total lipid occurred at a mean rate of 0.484±0.083 nmol/kg per min (n = 7), or ~0.6% of the sodium-dependent 2-[^{3}H]*myo*-inositol uptake of 77.0±10.2 nmol/kg per min (n = 7) measured in the same tissue samples.

DISCUSSION

The free *myo*-inositol concentration in mammalian peripheral nerve, which normally exceeds that in plasma by 90–100-fold, (15, 17, 37, 38) is significantly and reproducibly reduced by experimental diabetes (4, 15–17, 37) as a consequence of insulin deficiency and/or hyperglycemia (15). The present studies explore the possibility that *myo*-inositol uptake by endoneurial tissue contributes to the high steady-state tissue concentration of *myo*-inositol in peripheral nerve and that altered ambient insulin or glucose concentration directly influences this uptake process.

2-[^{3}H]*myo*-inositol uptake was examined under metabolically defined conditions in a metabolically stable peripheral nerve tissue preparation (3, 27) whose free *myo*-inositol concentration is reduced by acute experimental diabetes (4). 10-min periods of 2-[^{3}H]*myo*-inositol uptake were used to estimate unidirectional flux from the medium into the tissue preparation under various incubation conditions. The results demonstrate that uptake occurs by at least two distinct transport systems. A sodium-dependent transport system is responsible for ~94% of the measured uptake at medium *myo*-inositol concentrations approximating that present in plasma (endoneurial fluid *myo*-inositol concentration is unknown). The sodium dependency is absolute since saturable 2-[^{3}H]*myo*-inositol uptake is effectively abolished within 15 min in a sodium-free medium (the ability of other small ions to substitute for sodium was not assessed). Sodium-dependent *myo*-inositol uptake demonstrates relative specificity, since it is inhibited in a primarily competitive fashion by structurally-similar D-glucose, but not by mannitol or fructose. Saturability and stereospecificity would indicate that this uptake process is carrier-mediated. The sodium-dependent component of 2-[^{3}H]*myo*-inositol uptake is linear with respect to time, and demonstrates classical Michaelis-Menten kinetics. The transport carrier has a high affinity for *myo*-inositol, with an apparent K_t of 82.5 μM in the presence of 5 mM glucose, 63.3 μM in the absence of glucose, and 114 μM in the presence of 20 mM glucose (Table I). The resultant apparent $K_{i(glucose)}$ of 37.8 mM implies an apparent affinity of the carrier for *myo*-inositol ~500 times stronger than for glucose.

Carrier-mediated 2-[^{3}H]*myo*-inositol uptake by the endoneurial preparation is tightly linked to the sodium-ion electrochemical gradient at the plasma membrane since uptake is impaired by conditions which either raise intracellular sodium (ouabain) or lower extracellular sodium (choline buffer). Metabolite-concentrating transport systems in animal cell plasma membranes uniformly depend on electrochemical gradients generated by membrane ion pumps for

their energy source (39). The sodium-gradient dependence and apparent irreversibility of carrier-mediated 2-[^{3}H]*myo*-inositol uptake suggest *myo*-inositol concentrating capacity. (It is unlikely that nonmediated sodium-independent transport functions in this fashion since it is readily reversible). The recovery of virtually all tissue ^{3}H in a water soluble, nonvolatile and nonpolar moiety excludes intracellular accumulation of 2-[^{3}H]*myo*-inositol phosphates or phosphoinositides, or metabolism of 2-[^{3}H]*myo*-inositol to *myo*-inosose-2 (releasing ^3H_2O) as the basis of the irreversible carrier-mediated entry of ^{3}H.

The endoneurial preparation demonstrates a stable, high tissue *myo*-inositol concentration, little *myo*-inositol efflux during incubation in *myo*-inositol-free medium, absence of obvious intracellular *myo*-inositol binding capacity, and a sodium- and energy-dependent, irreversible carrier-mediated transport system for *myo*-inositol. Sodium-dependent endoneurial *myo*-inositol transport resembles saturable uptake systems in other tissues thought to concentrate *myo*-inositol, e.g., brain (40), lens (25, 41), choroid plexus (36, 42), ciliary body (24), small intestine (22), and kidney tubules (21, 22, 43). Taken together, these observations suggest that carrier-mediated transport contributes to the maintenance of high *myo*-inositol concentrations in some endoneurial components(s). Although the transport V_{max} is low, a slow-leak hypothesis has been invoked to reconcile high tissue-to-plasma *myo*-inositol concentration gradients with low *myo*-inositol transport capacity in other tissues (25). The stability of the endoneurial intracellular *myo*-inositol concentration during incubation in *myo*-inositol-free medium is consistent with this hypothesis, i.e., the existence of a slow-leak of *myo*-inositol from the normal endoneurial preparation. Implicit in the slow-leak hypothesis, however, is the prediction that independent factors that influence passive efflux may prominently affect steady-state tissue-to-plasma concentration gradients.

The physiological significance of glucose-mediated inhibition of *myo*-inositol uptake would depend on at least two factors: (*a*) the quantitative contribution of sodium-dependent uptake to the maintenance of high tissue *myo*-inositol concentrations, and (*b*) the relative concentrations of glucose and *myo*-inositol in endoneurial fluid. Neither *myo*-inositol pool size nor synthetic or metabolic flux is sufficiently well characterized in peripheral nerve to permit meaningful quantitative comparison with sodium-dependent *myo*-inositol uptake (17, 18, 26, 42, 44, 45). Moreover, endoneurial fluid *myo*-inositol concentration, which may possibly differ from that of plasma (46, 47), is unknown. However, both in vivo (48) and in vitro (3) experiments suggest that endoneurial fluid glucose freely equilibrates with plasma glucose and should therefore reflect plasma glucose concentration. Unequivocal evaluation of the physiological relevance of glucose-mediated inhibition of sodium-dependent *myo*-inositol uptake in diabetic peripheral nerve must await reliable endoneurial fluid sampling techniques.

Furthermore, the endoneurial preparation is a composite of heterogeneous cell types, primarily myelinated and unmyelinated axons and their accompanying Schwann cells (27). Free *myo*-inositol is highly and selectively concentrated within specific cell populations in brain, and a similarly heterogeneous distribution may occur in peripheral nerve (49). Since the high tissue level of *myo*-inositol in peripheral nerve has been variously attributed by indirect means to both the axon (50) and the Schwann cell (38), cellular localization of sodium-dependent *myo*-inositol uptake within peripheral nerve remains controversial.

The present studies describe a saturable, carrier-mediated sodium- and energy-dependent transport system for *myo*-inositol in the endoneurial preparation. Uptake by this system is not acutely influenced by physiologic concentrations of insulin, but is inhibited by hyperglycemic concentrations of glucose in a primarily competitive fashion. In view of the consistent and physiologically significant reduction in steady-state peripheral nerve *myo*-inositol content produced by experimental diabetes, it is reasonable to hypothesize (*a*) that carrier-mediated *myo*-inositol uptake contributes to the maintenance of high tissue *myo*-inositol levels within some component of peripheral nerve, and (*b*) that hyperglycemia reduces this concentration of free *myo*-inositol in part by competitively inhibiting sodium-dependent *myo*-inositol uptake. Thus, inhibition of peripheral nerve *myo*-inositol uptake by glucose constitutes a mechanism by which hyperglycemia may directly induce a specific metabolic alteration that has been implicated in impaired tissue function in experimental (15, 16) and human (51–53) diabetes.

ACKNOWLEDGMENTS

The authors wish to express their gratitude to Ms. Lorraine Lofink and Mr. Timothy McNulty for expert technical assistance, to Ms. Brenda O'Donnell for typing the manuscript, to Drs. David Finegold, Irwin Klein, Stephen Kempson, and Carlos Portocarrero for reviewing the manuscript, and to Dr. Rex Clements for his helpful comments during the studies herein reported.

The studies were supported in part by the Harry Soffer Memorial Research Fund and U. S. Public Health Service research grant R01-AM2982.

REFERENCES

1. Field, R. A., and L. C. Adams. 1964. Insulin response of peripheral nerve. I. Effects on glucose metabolism and permeability. *Medicine (Baltimore).* **43:** 275–279.
2. Field, R. A., and L. C. Adams. 1965. Insulin response

of peripheral nerve. II. Effects on lipid metabolism. *Biochim. Biophys. Acta.* **106:** 474–479.
3. Greene, D. A., and A. I. Winegrad. 1979. In vitro studies of the substrates for energy production and the effects of insulin on glucose utilization in the neural components of peripheral nerve. *Diabetes.* **28:** 878–887.
4. Greene, D. A., and A. I. Winegrad. 1981. Effects of acute experimental diabetes on composite energy metabolism in peripheral nerve axons and Schwann cells. *Diabetes.* **30:** 976–974.
5. Spritz, N., H. Singh, and B. Marinan. 1975. Metabolism of peripheral nerve myelin in experimental diabetes. *J. Clin. Invest.* **55:** 1049–1056.
6. Graf, R. J., J. B. Halter, E. Halar, and D. Porte. 1979. Nerve conduction abnormalities in untreated maturity-onset diabetes: relation to levels of fasting plasma glucose and glycosylated hemoglobin. *Ann. Intern. Med.* **90:** 298–303.
7. Clements, R. S. 1979. Diabetic neuropathy: new concepts of its etiology. *Diabetes.* **28:** 604–611.
8. Day, J. F., S. R. Thorpe, and J. W. Baynes. 1979. Nonenzymatically glycosylated albumin. In vitro preparation and isolation from normal human serum. *J. Biol. Chem.* **254:** 595–597.
9. Shapiro, R., M. J. McManus, C. Zalut, and H. F. Bunn. 1980. Site of nonenzymatic glucosylation of human hemoglobin A. *J. Biol. Chem.* **255:** 3120–3127.
10. Rosenberg, H., J. B. Modrak, J. M. Hassing, W. A. Al-Turk, and S. J. Stohs. 1979. Glycosylated collagen. *Biochem. Biophys. Res. Commun.* **91:** 498–501.
11. Pande, A., W. H. Garner, and A. Spector. 1979. Glycosylation of human lens protein and cataractogenesis. *Biochem. Biophys. Res. Commun.* **89:** 1260–1266.
12. Miller, J. A., E. Gravallese, and H. B. Bunn. 1980. Nonenzymatic glucosylation of erythrocyte membrane proteins. *J. Clin. Invest.* **65:** 896–901.
13. Schnider, S. L., and R. R. Kohn. 1980. Glucosylation of human collagen in aging and diabetes mellitus. *J. Clin. Invest.* **66:** 1179–1181.
14. Vlassara, H., M. Brownlee, and A. Cerami. 1981. Nonenzymatic glycosylation of peripheral nerve protein in diabetes mellitus. *Proc. Natl. Acad. Sci. U. S. A.* **78:** 5190–5192.
15. Greene, D. A., P. V. DeJesus, Jr., and A. I. Winegrad. 1975. Effects of insulin and dietary myoinositol on impaired peripheral motor nerve conduction velocity in acute streptozotocin diabetes. *J. Clin. Invest.* **55:** 1326–1336.
16. Greene, D. A., R. A. Lewis, M. J. Brown, S. A. Lattimer. 1982. Selective effects of *myo*-inositol administration on sciatic and tibial motor nerve conduction parameters in the streptozocin-diabetic rat. *Diabetes.* **31:** 573–578.
17. Clements, R. S., and C. R. Stockard. 1980. Abnormal sciatic nerve *myo*-inositol metabolism in the streptozotocin-diabetic rat. *Diabetes.* **29:** 227–235.
18. Hothersall, J. S., and P. McLean. 1979. Effect of experimental diabetes and insulin on phosphatidyl-inositol synthesis in rat sciatic nerve. *Biochem. Biophys. Res. Commun.* **88:** 477–484.
19. Dawson, R. M. C., and N. Freinkel. 1960. The distribution of free mesoinositol in mammalian tissues, including some observations on the lactating rat. *Biochem. J.* **78:** 606–610.
20. Molitoris, B. A., I. E. Karl, and W. H. Daughaday. 1980. Concentration of *myo*-inositol in skeletal muscle of the rat occurs without active transport. *J. Clin. Invest.* **65:** 783–788.
21. Hammerman, M. R., B. Sacktor, and W. H. Daughaday. 1980. Myo-inositol transport in renal brush border vesicles and its inhibition by D-glucose. *Am. J. Physiol.* **239:** F113–F120.
22. Caspary, W. F., and R. K. Crane. 1970. Active transport of myo-inositol and its relation to the sugar transport system in hamster small intestine. *Biochim. Biophys. Acta.* **203:** 308–316.
23. Spector, R., and A. V. Lorenzo. 1975. The origin of myo-inositol in brain, cerebrospinal fluid, and choroid plexus. *J. Neurochem.* **25:** 353–354.
24. Reddy, V. N., S. D. Varma, and B. Chakrapani. 1970. Intraocular transport of myoinositol. I. Accumulation in the rabbit ciliary body. *Invest. Ophthalmol.* **9:** 785–793.
25. Cotlier, E. 1970. Myo-inositol: active transport by the crystalline lens. *Invest. Ophthalmol.* **9:** 681–691.
26. Stewart, M. A., W. R. Sherman, and J. T. Harris. 1969. Effects of galactose on levels of free myo-inositol in rat tissues. *Ann. N. Y. Acad. Sci.* **165:** 609–614.
27. Greene, D. A., A. I. Winegrad, J-L. Carpentier, M. J. Brown, M. Fukuma, and L. Orci. 1979. Rabbit sciatic nerve fascicle and 'endoneurial' preparations for in vitro studies of peripheral nerve glucose metabolism. *J. Neurochem.* **33:** 1007–1018.
28. Chen, R. F. 1967. Removal of fatty acids from serum albumin by charcoal treatment. *J. Biol. Chem.* **25:** 173–181.
29. Ferrendelli, J. A., E. H. Rubin, H. T. Orr, D. A. Kinscherf, and O. H. Lowry. 1977. Measurement of cyclic nucleotides in histologically defined samples of brain and retina. *Anal. Biochem.* **78:** 252–259.
30. Barnett, J. E. G., R. E. Brice, and D. L. Corina. 1970. A colorimetric determination of inositol monophosphates as an assay for D-glucose 6-phosphate-1L-myo-inositol 1-phosphate cyclase. *Biochem. J.* **119:** 183–186.
31. Peach, D. M., and J. C. Russell. 1977. A binding protein from rat nerve. *Physiol. Chem. Phys.* **9:** 227–240.
32. Hauser, G., and J. Eichberg. 1973. Improved conditions for the preservation and extraction of polyphosphoinositides. *Biochim. Biophys. Acta.* **326:** 201–209.
33. Folch, J., M. Lees, S. G. H. Sloan. 1957. A simple method for the isolation and purification of total lipids from animal tissue. *J. Biol. Chem.* **226:** 497–509.
34. Lowry, O. H., and J. V. Passonneau. 1972. A Flexible System of Enzymatic Analysis. Academic Press, Inc., New York. 123.
35. Sokal, R. R., and F. J. Rohlf. 1969. Biometry: The Principles and Practice of Statistics in Biological Research. W. H. Freeman & Co., San Francisco.
36. Spector, R. 1976. The specificity and sulfhydryl sensitivity of the inositol transport system of the central nervous system. *J. Neurochem.* **27:** 229–236.
37. Palmano, K. P., P. H. Whiting, and J. N. Hawthorne. 1977. Free and lipid myoinositol in tissues from rats with acute and less severe streptozotocin-induced diabetes. *Biochem. J.* **167:** 229–235.
38. Kusama, H., and M. A. Stewart. 1970. Levels of myo-inositol in normal and degenerating peripheral nerve. *J. Neurochem.* **17:** 317–323.
39. Kyte, J. 1981. Molecular considerations relevant to the mechanism of active transport (review article). *Nature (Lond.).* **16:** 201–204.
40. Spector, R. 1976. Inostiol accumulation by brain slices in vitro. *J. Neurochem.* **27:** 1273–1276.
41. Varma, S. D., B. Chakarpani, and V. N. Reddy. 1970. Intraocular transport of myoinositol. II. Accumulation

in the rabbit lens in vitro. *Invest. Ophthalmol.* **9:** 794–800.
42. Mauck, L. A., Y-H. Wong, and W. R. Sherman. 1980. L-myo-inositol-1-phosphate synthase from bovine testis: purification to homogeneity and partial characterization. *Biochemistry.* **19:** 3623–3629.
43. Beck, J. C., and B. Sacktor. 1975. Energetics of the Na^+-dependent transport of D-glucose in renal brush border membrane vesicles. *J. Biol. Chem.* **250:** 8647–8680.
44. Whiting, P. H., K. P. Palmano, and J. N. Hawthorne. 1979. Enzymes of myo-inositol and inositol lipid metabolism in rats with streptozotocin-induced diabetes. *Biochem. J.* **179:** 549–553.
45. Sherman, W. R., M. A. Stewart, M. M. Kurien, and S. L. Goodwin. 1968. The measurement of myo-inositol, myo-inosose-2 and scyllo-inositol in mammalian tissue. *Biochim. Biophys. Acta.* **158:** 197–205.
46. Olsson, Y. 1975. Vascular permeability in the peripheral nervous system. Peripheral Neuropathy, Volume I, P. Dyck, P. K. Thomas and E. M. Lambert, editors. 190–200.
47. Spector, R., and A. V. Lorenzo. 1975. Myo-inositol transport in the central nervous system. *Am. J. Physiol.* **228:** 1510–1518.
48. Stewart, M. A., W. R. Sherman, M. M. Kurien, G. I. Moonsammy, and M. Wisgerhof. 1967. Polyol accumulations in nervous tissue of rats with experimental diabetes and galactosaemia. *J. Neurochem.* **14:** 1057–1066.
49. Sherman, W. R., P. M. Packman, M. H. Laird, and R. L. Boshans. 1977. Measurement of *myo*-inositol in single cells and defined areas of the nervous system by selected ion monitoring. *Ann. Biochem.* **78:** 119–131.
50. Gould, R. 1976. Inositol lipid synthesis localized in axons and unmyelinated fibers of peripheral nerve. *Brain Res.* **117:** 169–174.
51. Clements, R. S., Jr., B. Vourganti, T. Kuba, S. J. Oh, and B. Darnell. 1979. Dietary myo-inositol intake and peripheral nerve function in diabetic neuropathy. *Clin. Endocrinol. Metab.* **28:** 477–483.
52. Salway, J. G., J. A. Finnegan, D. Barnett, L. Whitehead, A. Karunanayaka, and R. B. Payne. 1978. Effects of myoinositol on peripheral nerve function in diabetes. *Lancet.* **II:** 1282–1284.
53. Greene, D. A., M. J. Brown, S. N. Braunstein, S. S. Schwartz, A. K. Asbury, and A. I. Winegrad. 1981. Comparison of clinical course and sequential electrophysiological tests in diabetics with symptomatic polyneuropathy and its implications for clinical trials. *Diabetes.* **30:** 139–147.